haematologica
Journal of the Ferrata Storti Foundation

Mutational and copy number analysis at diagnosis and relapse of mantle cell lymphoma

by Erel Joffe, Manik Uppal, Serena Zheng, Kurt S. Bantilan, Connie Batlevi, Zachary Epstein-Peterson, Paola Ghione, Paul Hamlin, Matthew Matasar, Alison Moskowitz, Ariela Noy, Maria L. Palomba, Gottfried Von Keudell, Lorenzo Falchi, Joachim Yahalom, Vitaly Segodin, Nikita Kotlov, Evgeniy Egorov, Sandrine Degryse, Aleksander Bagaev, Nathan Fowler, Maria Arcila, Ahmet Dogan, Gilles Salles, Anita Kumar and Andrew Zelenetz

Received: January 11, 2025.
Accepted: November 17, 2025.

Citation: Erel Joffe, Manik Uppal, Serena Zheng, Kurt S. Bantilan, Connie Batlevi, Zachary Epstein-Peterson, Paola Ghione, Paul Hamlin, Matthew Matasar, Alison Moskowitz, Ariela Noy, Maria L. Palomba, Gottfried Von Keudell, Lorenzo Falchi, Joachim Yahalom, Vitaly Segodin, Nikita Kotlov, Evgeniy Egorov, Sandrine Degryse, Aleksander Bagaev, Nathan Fowler, Maria Arcila, Ahmet Dogan, Gilles Salles, Anita Kumar and Andrew Zelenetz. Mutational and copy number analysis at diagnosis and relapse of mantle cell lymphoma. Haematologica. 2025 Nov 27. doi: 10.3324/haematol.2024.286813 [Epub ahead of print]

Mutational and copy number analysis at diagnosis and relapse of mantle cell lymphoma

Erel Joffe[1], Manik Uppal[1,2], Serena Zheng[1], Kurt S. Bantilan[1], Connie Batlevi[1], Zachary Epstein-Peterson[1,2], Paola Ghione[1,2], Paul Hamlin[1,2], Matthew Matasar[1], Alison Moskowitz[1,2], Ariela Noy[1,2], Maria L. Palomba[1,2], Gotfried Von Keudell [1], Lorenzo Falchi [1,2], Joachim Yahalom [1,2], Vitaly Segodin[3], Nikita Kotlov[3], Evgeniy Egorov[3], Sandrine Degryse[3], Aleksander Bagaev[3], Nathan Fowler[3], Maria Arcila [1,2], Ahmet Dogan[1,2], Gilles Salles[1,2], Anita Kumar[1,2*], and Andrew D. Zelenetz[1,2*]

Running title: Mutational landscape of MCL: diagnosis and relapse

1 Memorial Sloan Kettering Cancer Center, Department of Medicine, New York NY, USA
2 Weill Cornell College of Medicine, New York NY, USA
3 BostonGene, Corporation. Waltham MA, USA

Co-corresponding authors:
Erel Joffe MD, Memorial Sloan Kettering Cancer Center, Department of Medicine. 530 East 74th Street, New York, NY 10021. erelj@tlvmc.gov.il

Andrew D. Zelenetz, MD PhD, Memorial Sloan Kettering Cancer Center, 530 East 74th Street, New York, NY 10021. zeleneta@mskcc.org

*Co-senior authors

Key points: This study sought to identify genomic alterations associated with progression in MCL by analyzing tumor specimens from a large cohort of patients sequenced prior to initiation of frontline treatment or at the time of progression, including a subset of patients with sequential samples.

Our findings suggest that MCL relapse is predominantly driven by pre-existing malignant clones at diagnosis, rather than by new evolutionary events, underscoring the importance of early detection and eradication of resistant clones to improve long-term outcomes.

Key words: mantle cell lymphoma; cytogenetics and molecular genetics; genomic evolution.

FUNDING

This research was funded in part through the NIH/NCI Cancer Center Support Grant P30 CD008748 and SPORE grant 5 P50 CA192937.

AUTHORSHIP CONTRIBUTIONS

EJ, AZ, AK designed the research; VS, NK, EE, SD, AB, NF developed and optimized the copy number alteration call algorithm. EJ, MU, SZ, KB collected the data; EJ performed the biostatistical analyses and wrote the manuscript; EJ, CB, ZEP, PG, PH, MM, AM, AN, ALP, VKG, FL, YJ, GS, AK, AZ enrolled subjects and provided clinical data; MA, AD provided targeted sequencing support; All authors reviewed and approved the manuscript.

CONFLICT OF INTEREST DISCLOSURES

EJ: Honoraria Abbvie, Janssen. MLP: Honoraria: Pharmacyclics, Celgene, Merck, Novartis, Regeneron, Juno Therapeutics, a Bristol-Meyers Squibb Company: Research Funding; Genentech, Juno Therapeutics. AN: Research funding: Rafael Pharma, Pharmacyclics; Consultancy: Pharmacyclics, Medscape, Targeted Oncology, Morphosys, Pharmacyclics, Janssen; Research Funding; NIH. MM: Consultancy, Honoraria, Research Funding: Genentech, Inc, Bayer, Immunovaccine; Consultancy: Merck, Bayer, Juno Therapeutics, F. Hoffmann-La Roche Ltd; Technologies, Daiichi Sankyo, Seattle Genetics: Consultancy, IGM Biosciences, Janssen, Pharmacyclics, Rocket Medical, Takeda, GlaxoSmithKline, Teva. PH: Research Funding: J&J Pharmaceuticals, Portola, Molecular Templates, Incyte; Consultancy: Celgene, Karyopharm, Juno Therapeutics. CLB: Employment Genetech; AK: Honoraria: Kite Pharmaceuticals, Astra Zeneca, Celgene, Seattle Genetics: Research Funding; Pharmacyclics, Celgene, Adaptive Biotechnologies, AbbVie. AM: Consultancy: Seattle Genetics, Miragen Therapeutics, Imbrium Therapeutics, L.P., Merck: Research Funding; Bristol-Myers Squibb, Incyte, Seattle Genetics, Merck. LF: Research Funding: Genmab, Roche. GvK: Consultancy, Honoraria: Merck. AD: Consultancy: Takeda, Roche; Research Funding: Physicians Education Resource, Corvus Pharmaceuticals, Seattle Genetics, EUSA Pharma, AbbVie, National Cancer Institute. AZ: Board of Directors or advisory committees: BeiGene; Consultancy: Adaptive Biotechnology, Novartis, Amgen, Janssen, Celgene, Gilead, Genentech/Roche, Gilead; Research Funding: Roche, Celgene, Sandoz, MorphoSys, MEI Pharma. Employees of BostoneGene: VS, NK, EE, SD, AB, NF.

DATA SHARING

Clinical and molecular data can be made available upon request

ABSTRACT

Most patients diagnosed with mantle cell lymphoma (MCL) experience extended remissions following frontline chemoimmunotherapy, yet with with extended follow-up, relapses seem nearly inevitable. This study aimed to define the genomic landscape of MCL at diagnosis and relapse and investigate the clonal evolutionary dynamics associated with progression of disease (POD).

We conducted comprehensive genomic sequencing on 214 tumor specimens from 189 patients, including 144 treatment-naïve and 70 POD samples, with 25 patients providing longitudinal paired samples pre-treatment and at POD. Comparative analyses were performed on single nucleotide variants (SNVs), insertions/deletions (indels), and copy number alterations (CNAs) to assess genomic differences between treatment-naïve and relapsed specimens. Additionally, mutational signatures were evaluated in pre-treatment samples, stratified by time to progression (≤24 months vs. >24 months). One hundred patients who received standard frontline chemoimmunotherapy were included in the survival analysis.

Genomic profiles of pre-treatment specimens from patients who ultimately relapsed were strikingly similar to those observed in POD, while distinctly different from profiles associated with prolonged remissions. This genomic ‘stability’ was further confirmed by analysis of 25 paired specimens, demonstrating a remarkable genomic concordance despite extended remission periods (median >3 years), without a clear pattern of acquired alterations

Our findings suggest that MCL relapse is predominantly driven by pre-existing malignant clones at diagnosis, rather than by new evolutionary events, underscoring the importance of early detection and eradication of resistant clones to improve long-term outcomes.

INTRODUCTION

Most patients diagnosed with mantle cell lymphoma (MCL) typically experience long remissions following frontline chemoimmunotherapy.[1,2] However, with extended follow-up, relapses appear almost inevitable, and are associated with progressively shorter remissions to subsequent therapies.[3–5] This ultimate shift in disease course suggests an acquired molecular event that promotes to the emergence of a prevailing resistant clone.[6] Consequently, understanding the evolutionary processes that occur during these extended remissions is a priority.

Our understanding of the genomic evolution of MCL remains limited. [6–8] Similar to other lymphomas, two primary patterns of progression have been suggested.[6] The first includes primary refractoriness and early relapses, frequently characterized by persistent minimal residual disease.[9] The second pattern, is associated with prolonged MRD-negative remissions.[6,7] The only abnormalities that have consistently predicted inferior responses and shorter remissions across studies have been mutations in *TP53*. However, these account for fewer than half of POD events, leaving many cases unexplained.[10,11] Additional genomic alterations suggested to confer a poorer prognosis are mutations in *KMT2D* and deletions at the *CDKN2A* locus.[12,13] In particular, it appears, that copy number alterations (CNAs) play a pivotal role in the disease course of MCL.[13] Notably, two prior studies on small cohorts of MCL with sequential samples before and after frontline treatment demonstrated a subset of patients acquiring CNAs, primarily affecting *CDKN2A*. However, there was no definite acquisition of abnormalities to clearly support an evolutionary process.[6,7]

This study sought to identify genomic alterations associated with progression in MCL and to evaluate whether an identifiable evolutionary process underlies lymphoma persistence along the continuum of care. To achieve this, we studied tumor specimens from a large cohort of MCL patients who were sequenced either prior to initiation of frontline treatment or at the time of progression, including a subset of patients with sequential samples.

METHODS

This study analyzed data from patients diagnosed with MCL who underwent tumor specimen sequencing during their disease course. Sequencing was conducted in a CLIA-certified laboratory at Memorial Sloan Kettering Cancer Center using the institutional targeted sequencing platform, IMPACT-HEME. The study received Institutional Review Board approval, and all patients provided informed consent.

Targeted sequencing

Following consent, archival or new tumor biopsy samples were sequenced with saliva or nails used as a source of normal control (germline) DNA.[14] The MSK-IMPACT platform, a hybridization capture-based assay, was used to sequence all protein-coding exons of 399 cancer-associated genes on the Illumina HiSeq2500 (Table S1). Average sequencing coverage across all tumors was 748-fold. Paired-sample variant calling identified single nucleotide variants (SNVs) and small indels (<30 bp) in tumor samples matched with normal controls.[14]

Identification of copy number alterations

CNA analysis used a modified version of Sequenza v2.1.2, optimized by BostonGene to minimize focal false-positive segments particularly in centromere regions. FACETS v0.5.14 SNP database provided comprehensive extraction coverage. Given the limited heterozygous loci in the targeted sequencing approach, Strelka2 v2.8.2 germline caller was used to identify heterozygous variants, which were incorporated into individual reference files, improving statistical segmentation and CNA calling. CNAs were limited to genes validated by SNP array and described in the literature (Supplementary figures S1 and S2). CNAs were limited to genes validated by cases with available SNP array data (N=18; Table S2) and those described in the literature.

Clustering, prognostic features and survival analyses

To identify tumors with shared genetic features we applied hierarchical clustering with Jaccard distances and Ward linkage. We selected this approach as it is particularly suited for asymmetric binary data and offers the added advantage of intuitive dendrogram visualization.[15] We compared genomic features between samples grouping on time of sequencing (pre-treatment vs. relapse) and stratified by Ki67 proliferation index (<30%, 30–59%, ≥60%). We further sub-

divided the pre-treatment group to POD24 (progression of disease ≤24m post-therapy, and LR (long remission - those with a follow-up ≥24m without progression) and compared to samples at relapse. For sequential samples, a minimum of three months elapsed between frontline treatment initiation and the relapse sample. For patients with multiple relapse samples, the earliest specimen was selected. Only patients sequenced prior to standard frontline chemoimmunotherapy were included in survival analyses. Patients with concurrent malignancies (apart from low-grade or non-life-threatening cancers) were excluded.

Statistical analysis

Genomic abnormality frequencies were compared between groups using the Fisher exact test; paired samples were analyzed with McNemar and t-tests. Kaplan-Meier survival analysis and the log-rank test evaluated progression-free and overall survival (PFS/OS), calculated from treatment initiation to progression, death, or censoring. P-values and false discovery rate (FDR) corrections by Bonferroni-Hochberg were reported, with FDR significance set at $q < 0.1$. Analyses were conducted in R version 4.2.

Supplementary analyses included 125 additional samples excluded from the primary analysis for lack of validated CNA data. Of these, 99 were omitted due to informed consent restrictions preventing CNA assessment and 26 sequenced by FoundationHeme without use of individual matched-normal data.

RESULTS

We sequenced 334 samples from patients diagnosed with MCL. Of these, CNA data were available for 214 samples (189 unique patients; 88 cases excluded due to informed consent restrictions; 28 cases due to inadequate samples for CNA analysis). There were 144 patients sequenced prior to initiation of frontline therapy or while on expectant management and 70 patients were sequenced at the time of relapse (Table 1). Of these, 25 patients had samples sequenced prior to frontline treatment and at the time of relapse. One hundred patients were eligible for survival analysis (Figure 1; Supplementary figure S3 – expanded analysis n=321 without CNA data).

The most common genomic alterations were mutations in *ATM* (48%), *TP53* (28%), and *KMT2D* (22%). Gains or amplifications were observed in *TP63* (41%) and *MYC* (31%) and deletions were found in *RB1* (35%), *ATM* (34%), *CDKN2A* (28%), *ARID1B* (26%), and *TP53* (22%) (Figure 2; supplementary tables S3-4; figure S4 – expanded analysis without CNA data).

Deletions of *TP53* (17p13.1) co-occurred with mutations in *TP53* (65% of *TP53mut* were also *delTP53*; and 52% of *delTP53* were also *TP53mut*, $p<0.001$) and with amplification of *TP63* (3q28). The latter was also associated with mutations in *WHSC1* (*NSD2*) (Figure 3). Deletions of *ATM* (11q22.3) often co-occurred with mutations in either *ATM* or *BIRC3*, but not both (despite the proximity between the genes on the long arm of chromosome 11). Deletions of *TP53* and mutations of *TP53* were almost completely exclusive of deletions of *ATM* and mutations in *ATM* respectively. Deletions of *RB1* (13q14.2) co-occurred frequently with deletions of *ATM* (11q22.3), deletions of *CDKN2A* (9p21.3), deletions of *ARID1B* (6q25.3) and with mutations in *MEF2B*. *MEF2B* mutations were also mutually exclusive of amplifications of *MYC* (8q24.21) and mutations in *TP53*. Together, the above interactions generated three major clusters: the first converging around double-hit (deletion and mutation) in *ATM* (ATM-DH); the second around double-hit in *TP53* (TP53-DH) and the third characterized by absence of mutations in TP53 and of CNA in *TP53* and *ATM*, but with common mutations in *ATM* (ATM-MUT) (Figure 3).

There were 164 patients with follow-up of at least 24 months from initiation of treatment. Of these, 70 remained disease-free after frontline systemic therapy (LR) and 94 patients experienced a relapse (POD). Of the latter, 49 cases were sequenced prior to frontline therapy and 70 sequenced at relapse (25 patients contributed samples at two time points). The median time from sequencing prior to frontline therapy and POD was 21 months. Samples from patients who had ultimately experienced a POD, whether sequenced prior to frontline treatment or later, had higher rates of *TP53mut* (LR 10% vs. 33% for progressors sequenced prior to frontline therapy, and 42% for samples sequenced at subsequent lines of therapy, $p\leq0.001$), *delCDKN2A* (19% vs. 27% and 35%, $p\leq0.001$) and *delTP53* (11% vs. 24% and 28%, $p\leq0.001$) (Figure 4; table S3). Among the 49 patients sequenced pre-treatment whose lymphoma later progressed, there were 27 patients who experienced progression within the first 24 months from therapy initiation (POD24). Compared to samples sequenced prior to frontline therapy from patients who had long

remissions, samples from patients who later experienced a POD24 had numerically higher rates of *TP53* (44% vs. 12%, p=0.1) and *SMARCA4* mutations (26% vs. 9%, p=0.06, figure 4; figure S5 – expanded analysis mutation only). There was no significant difference in the variant allele frequency or number of mutations in any gene between patients sequenced at diagnosis and those at relapse (Table S3).

Twenty-five patients had sequential samples from pre-treatment and at time of POD/relapse. The median time between samples was 42m (IQR 18-51m). Acquisition or disappearance of genomic abnormalities, mostly CNA, were seen in 24 out of 25 patients; however, these were sporadic changes that were each present in very few patients (Figure 5; Supplementary figure S7A). Therefore, there was no statistically significant difference in the overall rate of genomic abnormalities between sequential samples nor was there a difference in the number of mutations per gene or in variant allele frequencies (Supplementary figure S6A and S7A and tables S5). The most common changes were the acquisition of an amp*CARD11* (6 pts), del*ATM* (4 pts), del*TP53* (4 pts), and del*CDKN2A* (4 pts). In 6 out of 8 patients, amp*CCND1* seen at diagnosis was not identified at the time of POD as was the case for *BIRC* mutations in 3 of 4 patients. *TP53* mutations were seen as a new event in only 2 patients and there was no difference in the genomic loci, number, or variant allele frequencies between pre-treatment and progression samples (Supplementary figure S6B; table S5). Of note, overall new events in the *TP53* gene were seen in 5 patients (2 of whom had *TP53* mutations at baseline and acquired a deletion).

There were 100 patients with samples sequenced prior to frontline treatment with chemoimmunotherapy, and eligible for survival analysis (table 2). Of these, 37% (n=37) experienced POD, half of whom experienced POD24. Though not statistically significant, patients who later experienced a POD were slightly older and with a higher rate of blastoid/high-Ki67 MCL compared to patients with long remissions. There was also a lower use of high-dose chemotherapy with stem cell support (ASCT; 24% vs. 59%, p=0.03) in this group. Most patients (75%) were treated with the intent to use intensive regimens. Median follow-up was nearly 5 years (57m; 95% CI 46-71m) with 95% of patients followed for at least 24 months (five patients

in remission who were followed for < 24m were excluded from analyses of long-remission). For LR patients the estimated 4y-PFS was 82% (95% CI 73-93%).

There were 22 patients whose MCL harbored a mutation in *TP53* and 20 patients with a deletion in *TP53* (of these, 12 had both a mutation and a deletion). A mutation in *TP53* was the only genomic abnormality associated with a shorter PFS in univariable and multivariable analyses (4y-PFS 26% vs. 76%, 95% CI 11-63% vs. 67-87%; HR 7.7; 95% CI 3-21, p<0.0001; q=0.002; table S6). This observation was also true for the subset of patients who proceeded to ASCT. The eight patients whose MCL harbored a deletion in *TP53* in the absence of a *TP53* mutation had a similar PFS as the *TP53wt* population (Figure 6; sample too small for statistical significance).

Overall, there were 63 patients in the entire cohort whose lymphoma harbored a mutation in *TP53* (46% sequenced prior to frontline, 32% at first relapse and 22% at later lines of therapy). Having demonstrated that mutations in *TP53* were an early event in MCL, we analyzed data for this cohort collectively (i.e., regardless of the time of sequencing). Patients with *TP53* mutated MCL had a lower response rate to frontline chemoimmunotherapy compared to *TP53wt*. Nonetheless most of these patients did display a response to treatment (ORR 76%; CR 59%). There were 65 patients who underwent an ASCT in first CR, of whom 16 had a *TP53* mutation. All but one patient with *TP53*-mutated MCL displayed a CR after ASCT; however, their PFS was considerably shorter than that of patients with *TP53-wt* (2y PFS 63% and 4y PFS 31% compared to 2y PFS 98% and 4y PFS 86%, p<0.0001, Figure 6).

DISCUSSION

We evaluated 214 samples from MCL patients sequenced either prior to frontline treatment (n=144) or at relapse (n=70). Samples from diagnosis from patients who ultimately progressed displayed a genomic profile, similar to that of samples sequenced at relapse and distinct from those of those with long remission. This trend was corroborated in 25 sequential samples, which showed similar profiles between pre-treatment and relapse samples, even when separated by a prolonged remission period (median remission time was >3 years). Notably, these acquired alterations did not follow a common pattern, though a trend toward acquisition of CNAs was observed. While recognizing the limitations of targeted sequencing and sample size, these

observations suggest that in most MCL cases, relapse is not driven by a uniform genomic evolution but rather by the persistence of resistant clones present at diagnosis.

Observed rates of SNV, indel, and CNA were consistent with those previously reported in retrospective MCL cohorts.[6,16,17] Notably, the observed rates of *TP53* and *CDKN2A* associated abnormalities in prospective clinical trials have been lower.[11,12,18] Importantly, a considerable variability in CNA rates across studies suggests that algorithmic criteria used to infer CNAs from NGS data contribute to these differences. Consequently, we made extensive efforts to optimize our CNA calling pipeline.

In keeping with our observation, in a recent study of sequential samples sequenced prior to frontline treatment and at POD, 9 out of 16 patients were noted to have newly acquired genomic abnormalities; however, these were primarily sporadic CNAs, each present in a single case.[6] The only repeatedly acquired CNAs (seen in three cases each) were deletions of 9p21.3-13.1 which includes *CDKN2A* and amplifications of 12q13.3-14.1 and which includes *CDK4* (not covered by our panel). As with our data, acquired deletion or mutation of *TP53* were only seen in one patient each, indicating this is an early event.[6,7] Similarly, in our sequential cohort, though not statistically significant, non-sporadic acquired abnormalities were limited to CNAs and included deletions of *CDKN2A* (9p21.3), *ATM* (11q22.3) and *TP53* (17p13.1) and amplifications of *CARD11* (7p22.2). [6,7] Interestingly, in 6 out of 8 patients with an amplification of *CCND1* (11q13.3), the abnormality was no longer evident at relapse. Though not statistically significant, higher rates of deletions in *CDKN2A* and *ATM* were seen when comparing pre-treatment samples of patients who later relapsed versus relapsed samples (a similar trend was not observed for *CCND1* amplifications), suggesting chromosomal instability may be a key evolutionary process in MCL.[7,17] This would further explain why relapsed samples were enriched for deletions in *CDKN2A,* yet this chromosomal abnormality was not prognostic in the frontline setting. Using hierarchical clustering we defined three major clusters which resemble those defined previously by Yi et. al.. The first cluster converged around double-hit (deletion and mutation) in *ATM* (corresponding to 'Cluster 2'); the second around double-hit in *TP53* (corresponding to 'Cluster 4') and the third characterized by common mutations in *ATM* in absence of mutations in *TP53* and of CNA in *TP53* and *ATM* (corresponding to 'Cluster 3'). Cluster 1 by Yi et. al. representing

non-nodal leukemic MCL was not captured, probably due to the smaller sample size and absence of IgHV status data in our clustering.

Samples from patients who ultimately experienced a POD, irrespective of whether the sequenced specimen was obtained at diagnosis or at relapse, exhibited considerably higher rates of genomic abnormalities in the apoptotic pathway, including mutations and deletions in *TP53* and *CDKN2A*. These abnormalities were particularly evident in cases with an early progression (<24m). As with prior studies, there was an incomplete overlap between *TP53* mutations and deletions, with *TP53* mutations emerging as the primary driver of dismal prognosis and accounting for nearly half of all relapses.[6,11,12] . Similarly, presence of a *TP53* mutation seems as a more specific predictor of dismal outcome compared to DH-TP53 cluster raising a question about the biological relevance of cluster allocation. There was no difference in the number or loci of *TP53* mutations between samples sequenced prior to frontline therapy or at POD.

Although a large proportion of patients with mutations in *TP53* initially achieved remission with standard chemoimmunotherapy, with many subsequently proceeding to ASCT, responses were generally short-lived, with nearly all patients experiencing progression within four years. Notably, however, most patients did demonstrate a significant response to frontline chemoimmunotherapy, an outcome that is relevant when considering the applicability of chemotherapy as a temporizing measurement when a rapid disease control is required.

The lack of a distinct pattern of acquired genomic abnormalities between diagnosis and relapse samples (noting the small proportion of cases showing acquisition of CNAs) suggests two predominant patterns of progression for MCL. In the more common scenario, a resistant clone or sub-clone present at diagnosis may persist for years even during so-called periods of remission eventually driving relapse. In the second scenario, which may be more prevalent in later relapses, a divergent evolution occurs, where a new clone drives progression, possibly originating from a precursor pre-malignant lymphoid clone.[19–21] The first scenario is supported by growing evidence linking undetectable minimal residual disease, as measured by ultra-sensitive techniques, with long-term remission.[9,22,23] The second scenario may be supported by findings that MCL-associated germline mutations occur in the general population and are linked to an

increased risk of MCL development with acquired chromosomal abnormalities.[20,21,24] In this context, divergent evolution in patients with delayed relapses has also been recently suggested in diffuse large B-cell lymphoma.[25]

Several limitations must be acknowledged that may impact the interpretation of our findings. Firstly, the lack of a formal tumor evolutionary analysis, such as phylogenetic reconstruction or clonal trajectory inference, may restrict our ability to conclusively determine whether relapse is solely driven by pre-existing clones identifiable at diagnosis. Further, our use of a targeted sequencing panel, rather than whole-exome or genome sequencing (WES/WGS) may have missed alterations outside the interrogated genes. Finally, the clinically diverse nature of our real-world patient population, which included individuals with varied backgrounds, disease presentations, and treatment regimens may have introduced a degree of heterogeneity that might confound specific associations between genotype and treatment response. Nonetheless, our findings are in keeping with previous cohorts of MCL in smaller more homogenous patient populations sequenced with WES/WGS, while targeted panels allowed us to achieve high sequencing depths, supporting sensitive detection of low-frequency variants including subclonal mutations that might be missed by less sensitive approaches.

Another limitation is that the size of our paired diagnosis-relapse cohort was limited (N=25), restricting statistical power for some evolutionary analyses. Notably, 5 out of 25 patients had new events in the *TP53* gene (2 of whom had *TP53* mutations at baseline and acquired a deletion) suggesting that, in a subset of patients, acquisition of new hits in the *TP53* gene may play a role in disease evolution under treatment pressure.[26] Notwithstanding, the striking genomic stability we observed in most pairs mirrors findings in chronic lymphocytic leukemia, diffuse large B cell lymphoma and follicular lymphoma where it has been shown that relapses are predominantly driven by selection of pre-existing resistant subclones.[27–30] We further recognize the absence of integrative multi omic studies such as single-cell RNA sequencing or methylation analysis that could reveal non genomic resistance mechanisms. In this regard, we invested substantial efforts into robust CNA calling, identifying accumulation of chromosomal changes that likely highlights the key role of genomic instability in MCL progression. Investigating other molecular mechanisms of progression would be of considerable interest but

was unfortunately beyond the scope of our present study. In fact, accumulating evidence suggests that drug tolerant states exist in absence of genetic evolution through mechanisms of phenotypic plasticity to resistant or quiescent states.[31]

CONCLUSIONS

In most patients with MCL, prognosis is primarily determined by malignant clones present at diagnosis, rather than by subsequent genomic evolution. In a subset of cases, however, acquisition of CNAs may suggest a form of genomic evolution likely driven by intrinsic abnormalities in apoptotic pathways characteristic of this malignancy.

REFERENCES

1. Le Gouill S, Thieblemont C, Oberic L, et al. Rituximab after Autologous Stem-Cell Transplantation in Mantle-Cell Lymphoma. N Engl J Med. 2017;377(13):1250-1260.
2. Hermine O, Hoster E, Walewski J, et al. Addition of high-dose cytarabine to immunochemotherapy before autologous stem-cell transplantation in patients aged 65 years or younger with mantle cell lymphoma (MCL Younger): a randomised, open-label, phase 3 trial of the European Mantle Cell Lymphoma Network. Lancet. 2016;388(10044):565-575.
3. Rule S, Dreyling M, Goy A, et al. Outcomes in 370 patients with mantle cell lymphoma treated with ibrutinib: a pooled analysis from three open-label studies. Br J Haematol. 2017;179(3):430-438.
4. Eyre TA, Walter HS, Iyengar S, et al. Efficacy of venetoclax monotherapy in patients with relapsed, refractory mantle cell lymphoma after Bruton tyrosine kinase inhibitor therapy. Haematologica. 2019;104(2):e68-e71.
5. Visco C, Di Rocco A, Evangelista A, et al. Outcomes in first relapsed-refractory younger patients with mantle cell lymphoma: results from the MANTLE-FIRST study. Leukemia. 2021;35(3):787-795.
6. Yi S, Yan Y, Jin M, et al. Genomic and transcriptomic profiling reveals distinct molecular subsets associated with outcomes in mantle cell lymphoma. J Clin Invest. 2022;132(3):e153283.
7. Karolova J, Kazantsev D, Svaton M, et al. Sequencing-Based Analysis of Clonal Evolution of 25 Mantle Cell Lymphoma Patients at Diagnosis and after Failure of Standard Immunochemotherapy. Blood. 2022;140(Supplement 1):6409-6410.
8. Holte H, Beiske K, Boyle M, et al. The MCL35 gene expression proliferation assay predicts high-risk MCL patients in a Norwegian cohort of younger patients given intensive first line therapy. Br J Haematol. 2018;183(2):225234.
9. Ladetto M, Tavarozzi R, Pott C. Minimal residual disease (MRD) in mantle cell lymphoma. Ann Lymphoma. 2020;4(0):4.
10. Eskelund CW, Dimopoulos K, Kolstad A, et al. Detailed Long-Term Follow-Up of Patients Who Relapsed After the Nordic Mantle Cell Lymphoma Trials: MCL2 and MCL3. Hemasphere. 2021;5(1):e510.
11. Eskelund CW, Dahl C, Hansen JW, et al. TP53 mutations identify younger mantle cell lymphoma patients who do not benefit from intensive chemoimmunotherapy. Blood. 2017;130(17):1903-1910.
12. Ferrero S, Rossi D, Rinaldi A, et al. KMT2D mutations and TP53 disruptions are poor prognostic biomarkers in mantle cell lymphoma receiving high-dose therapy: a FIL study. Haematologica. 2020;105(6):1604-1612.
13. Le Bris Y, Magrangeas F, Moreau A, et al. Whole genome copy number analysis in search of new prognostic biomarkers in first line treatment of mantle cell lymphoma. A study by the LYSA group. Hematol Oncol. 2020;38(4):446-455.
14. Ptashkin RN, Ewalt MD, Jayakumaran G, et al. Enhanced clinical assessment of hematologic malignancies through routine paired tumor and normal sequencing. Nat Commun. 2023;14(1):6895.
15. Coombes CE, Liu X, Abrams ZB, Coombes KR, Brock G. Simulation-derived best practices for clustering clinical data. J Biomed Inform. 2021;118:103788.

16. Nadeu F, Martin-Garcia D, Clot G, et al. Genomic and epigenomic insights into the origin, pathogenesis, and clinical behavior of mantle cell lymphoma subtypes. Blood. 2020;136(12):1419-1432.
17. Hartmann EM, Campo E, Wright G, et al. Pathway discovery in mantle cell lymphoma by integrated analysis of high-resolution gene expression and copy number profiling. Blood. 2010;116(6):953-961.
18. Freeman CL, Pararajalingam P, Jin L, et al. Molecular determinants of outcomes in relapsed or refractory mantle cell lymphoma treated with ibrutinib or temsirolimus in the MCL3001 (RAY) trial. Leukemia. 2022;36(10):2479-2487.
19. Pararajalingam P, Coyle KM, Arthur SE, et al. Coding and noncoding drivers of mantle cell lymphoma identified through exome and genome sequencing. Blood. 2020;136(5):572-584.
20. Petrackova A, Savara J, Turcsanyi P, Gajdos P, Papajik T, Kriegova E. Rare germline ATM variants of uncertain significance in chronic lymphocytic leukaemia and other cancers. Br J Haematol. 2022;199(3):371-381.
21. Lampson BL, Gupta A, Tyekucheva S, et al. Rare Germline ATM Variants Influence the Development of Chronic Lymphocytic Leukemia. J Clin Oncol. 2023;41(5):1116-1128.
22. Epstein-Peterson ZD, Batlevi CL, Caron P, et al. Frontline Sequential Immunochemotherapy Plus Lenalidomide for Mantle Cell Lymphoma Incorporating MRD Evaluation: Phase II, Investigator-Initiated, Single-Center Study. Blood. 2020;136(Supplement 1):11-12.
23. Lakhotia R, Melani C, Dunleavy K, et al. Circulating tumor DNA predicts therapeutic outcome in mantle cell lymphoma. Blood Adv. 2022;6(8):2667-2680.
24. Zhang J, Jima D, Moffitt AB, et al. The genomic landscape of mantle cell lymphoma is related to the epigenetically determined chromatin state of normal B cells. Blood. 2014;123(19):2988-2996.
25. Hilton LK, Ngu HS, Collinge B, et al. Relapse Timing Is Associated With Distinct Evolutionary Dynamics in Diffuse Large B-Cell Lymphoma. J Clin Oncol. 2023;41(25):4164-4177.
26. Agarwal R, Chan YC, Tam CS, et al. Dynamic molecular monitoring reveals that SWI–SNF mutations mediate resistance to ibrutinib plus venetoclax in mantle cell lymphoma. Nat Med. 2019;25(1):119-129.
27. Zapatka M, Tausch E, Öztürk S, et al. Clonal evolution in chronic lymphocytic leukemia is scant in relapsed but accelerated in refractory cases after chemo(immune) therapy. Haematologica. 2022;107(3):604-614.
28. Landau DA, Tausch E, Taylor-Weiner AN, et al. Mutations driving CLL and their evolution in progression and relapse. Nature. 2015;526(7574):525-530.
29. Burger JA, Landau DA, Taylor-Weiner A, et al. Clonal evolution in patients with chronic lymphocytic leukaemia developing resistance to BTK inhibition. Nat Commun. 2016;7:11589.
30. Bai B, Wise JF, Vodák D, et al. Multi-omics profiling of longitudinal samples reveals early genomic changes in follicular lymphoma. Blood Cancer J. 2024;14(1):147.
31. Pérez-González A, Bévant K, Blanpain C. Cancer cell plasticity during tumor progression, metastasis and response to therapy. Nat Cancer. 2023;4(8):1063-1082.

Table 1: Cohort characteristics

	All N=214	**Pre-treatment** N=144	**POD** N=70	**p value**
	N=214 (%)	N=144 (%)	N=70 (%)	
Age, years [IQR]	66 [58;72]	64 [57;71]	68 [61;75]	0.006
Sex (male), N (%)	168 (78.5%)	108 (75.0%)	60 (85.7%)	0.11
Timing of Sequencing, N (%)				
Prior to frontline	144 (67.3%)	144 (100%)		
First relapse/second line	44 (20.6%)		44 (62.9%)	
Second relapse/third line	18 (8.41%)		18 (25.7%)	
Multiply relapsed	8 (3.74%)		8 (11.4%)	
Features at the time of sequencing				
IgHV unmutated (n=77), N (%)	58 (75.3%)	35 (79.5%)	23 (69.7%)	0.47
del(17p) (by FISH/SNP; n=48) , N (%)	22 (45.8%)	11 (37.9%)	11 (57.9%)	0.29
Blastoid/pleomorphic, N (%)	42 (19.7%)	17 (11.9%)	25 (35.7%)	<0.001
Ki67 (n= 167) , N (%)				0.001
<30%	53 (31.7%)	43 (41.3%)	10 (15.9%)	
>=30%	71 (42.5%)	42 (40.4%)	29 (46.0%)	
>=60%	43 (25.7%)	19 (18.3%)	24 (38.1%)	

FISH – flurecense in-situ hybridization; IgHV – immunoglobulin heavy chain; POD – progression of disease; SNP – single nucleotide polymorphism array.

Table 2: Baseline characteristics survival-analysis cohort

	ALL	Long-remission	POD	Insufficient follow-up	p value
	N=100 (%)	N=58 (%)	N=37 (%)	N=5 (%)	
Age [IQR]	64 [57;71]	64 [56;68]	68 [56;72]	66 [63;72]	0.21
Sex (male)	66 (74.0%)	42 (72.4%)	28 (75.7%)	4 (80.0%)	0.93
ECOG > 1	96 (100%)	56 (100%)	35 (100%)	5 (100%)	
MIPI					0.39
Low-risk	34 (37.4%)	21 (39.6%)	11 (33.3%)	2 (40.0%)	
Intermediate-risk	37 (40.7%)	24 (45.3%)	11 (33.3%)	2 (40.0%)	
High-risk	20 (22.0%)	8 (15.1%)	11 (33.3%)	1 (20.0%)	
Stage					0.16
I	1 (1.00%)		1 (2.70%)		
II	7 (7.00%)	5 (8.62%)	1 (2.70%)	1 (20.0%)	
III	13 (13.0%)	5 (8.62%)	8 (21.6%)		
IV	79 (79.0%)	48 (82.8%)	27 (73.0%)	4 (80.0%)	
Spleen involvement	44 (45.4%)	26 (45.6%)	17 (48.6%)	1 (20.0%)	0.55
Bone marrow involvement	63 (69.2%)	39 (68.4%)	22 (73.3%)	2 (50.0%)	0.67
t(11;14) IGH:CCND1	96 (98.0%)	55 (96.5%)	36 (100%)	5 (100%)	0.57
Blastoid/pleomorphic	14 (14.0%)	6 (10.3%)	8 (21.6%)		0.26
Leukemic non nodal	6 (6.00%)	4 (6.90%)	2 (5.41%)		1.00
del17p (FISH/SNP)	6 (37.5%)	2 (20.0%)	4 (80.0%)		0.06
IgHV Unmutated	26 (81.2%)	10 (83.3%)	16 (84.2%)		0.24
Ki67					0.22
<30%	33 (40.2%)	18 (38.3%)	12 (40.0%)	3 (60.0%)	
30-59%	34 (41.5%)	23 (48.9%)	9 (30.0%)	2 (40.0%)	
>=60%	15 (18.3%)	6 (12.8%)	9 (30.0%)		
Frontline systemic treatment					
BR	23 (23.0%)	10 (17.2%)	11 (29.7%)	2 (40.0%)	
R-DHAX	18 (18.0%)	11 (19.0%)	4 (10.8%)	3 (60.0%)	
R2CHOP-RHDAC	20 (20.0%)	12 (20.7%)	8 (21.6%)		
RBAC	1 (1.00%)		1 (2.70%)		
RCHOP	3 (3.00%)		3 (8.11%)		
RCHOP / RDHAX	7 (7.00%)	4 (6.90%)	3 (8.11%)		
RCHOP / RHDAC	17 (17.0%)	13 (22.4%)	4 (10.8%)		
RCHOP / RICE	11 (11.0%)	8 (13.8%)	3 (8.11%)		
Primary refractory	11 (11.0%)		11 (29.7%)		<0.001
POD24	19 (19.0%)		19 (51.4%)		<0.001
ASCT (frontline)	45 (45.0%)	34 (58.6%)	9 (24.3%)	2 (40.0%)	0.003

ASCT – autologous hematopoietic stem cell transplant; BR – bendamustine rituximab; ECOG – Eastern cooperative oncology group performance status; FISH – flurecense in-situ hybridization; IgHV – immunoglobulin heavy chain; MIPI – mantle cell lymphoma international prognostic index; R2 – rituximab lenalidomide; RBAC – rituximab bendamustine cytarabine; RCHOP – rituximab cyclophophamide doxorubicin vincristine prednisone; RDHAC – rituximab high-dose cytarabine; R-DHAX – rituximab dexamethasone high-dose cytrarabine and oxaliplatin; RICE – rituximab ifosfamide carboplatin etoposide; POD24 – progression of disease within 24 months from initation of frontline therapy; SNP – single nucleotide polymorphism array.

Figure 1:

Consort Diagram - We sequenced 334 samples from patients diagnosed with MCL. Of these, CNA data was available for 214 samples (189 unique patients). 144 patients were sequenced prior to initiation of frontline therapy or while on expectant management and 70 patients were sequenced at the time of relapse. 100 patients were eligible for survival analysis.
* 25 patients were sequenced prior to frontline treatment and at the time of relapse.

Figure 2:

Genomic landscape of MCL (grouped by Ki67) - Genomic landscape of MCL for 189 unique patients (excluding repeated samples). Higher Ki67 associated with enrichment of TP53mut and deletions in RB1, CDKN2A, TP53 and ARID1A ($q<0.05$ after FDR correction; table S4).

Figure 3:

Genomic abnormalities association matrix and cluster analysis - Co-occurrence and mutual exclusivity of mutations and copy number alterations (A, C); genomic clusters by hierarchical clustering (B);
In table C – number of samples with both alterations present ('11'), both absent ('00') only one or the other present ('10'/'01').

Figure 4:

Genomic landscape at frontline and at later lines of treatment comparing patients with long remission to those with earlier progression of disease - Long Remission - follow-up of at least 24m without POD; Progression - disease relapse at any time (deaths without lymphoma not considered an event); Excluded are 49 samples of patients with insufficient follow-up or not treated with chemoimmunotherapy. (A) Samples prior to frontline therapy comparing patients with a long remission (>24m) to those of patients who experienced a relapse at any time; (B) Samples prior to frontline treatment from patients who experienced a POD24 (N=27) had a trend towards higher rates of TP53 and SMARCA4 mutations ($*p \leq 0.1$; not meeting statistical significance due to sample size); (C) samples sequenced at frontline from patients with POD24 were very similar to those sequenced at relapse; (D) Samples from patients sequenced at frontline who later experienced a POD24 and those sequenced at relapse had higher rate of mutations in SMARCA4 and lower rate of mutations in FAT1 ($*p < 0.05$; insignificant after correction for FDR).
Note: plots C&E exclude sequential samples from the same patient.

Figure 5:

Genomic landscape prior to frontline treatment and at POD (sequential samples) - Sequential samples where Time Seq (top_bottom_row) represent the timing of sequencing pre-treatment (light-green) or at the time of subsequent treatment, POD24 (second row) represents whether the first relapse occurred within 24 months (POD24 light-green) or whether the relapse occurred after a longer remission (LR light-blue). Thus, a combination of a light-blue box and a dark-green box on this line indicates a couplet of samples from before frontline treatment and after a considerable remission (the length of time between samples can be inferred from the bars at the top of the plot). Blastoid/Ki67 refers to disease status at the time of sequencing.

Figure 6:

Progression Free Survival by TP53 status and Cluster - Progression free survival from frontline chemoimmunotherapy treatment. (A) PFS by TP53 mutation and CNA status; (B) PFS by cluster; and (C) PFS of all patients undergoing frontline ASCT including patients sequenced prior to frontline therapy or at relapse (i.e. selection of patients who were fit to undergo an ASCT and who may have been sequenced at the time of a later relapse).

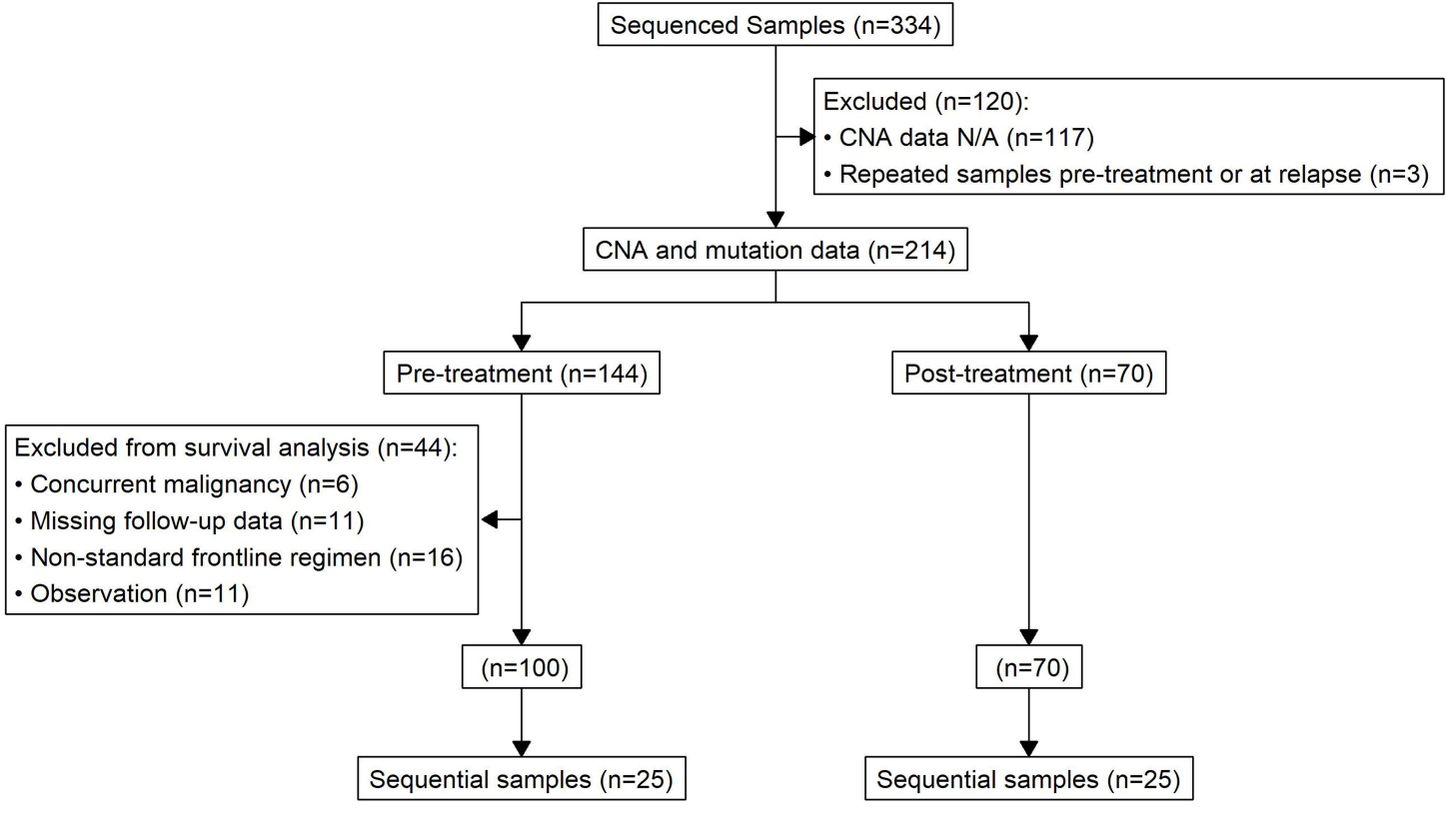
Sequenced Samples (n=334)
Excluded (n=120):
• CNA data N/A (n=117)
• Repeated samples pre-treatment or at relapse (n=3)
CNA and mutation data (n=214)
Pre-treatment (n=144)
Post-treatment (n=70)
Excluded from survival analysis (n=44):
• Concurrent malignancy (n=6)
• Missing follow-up data (n=11)
• Non-standard frontline regimen (n=16)
• Observation (n=11)
(n=100)
(n=70)
Sequential samples (n=25)
Sequential samples (n=25)

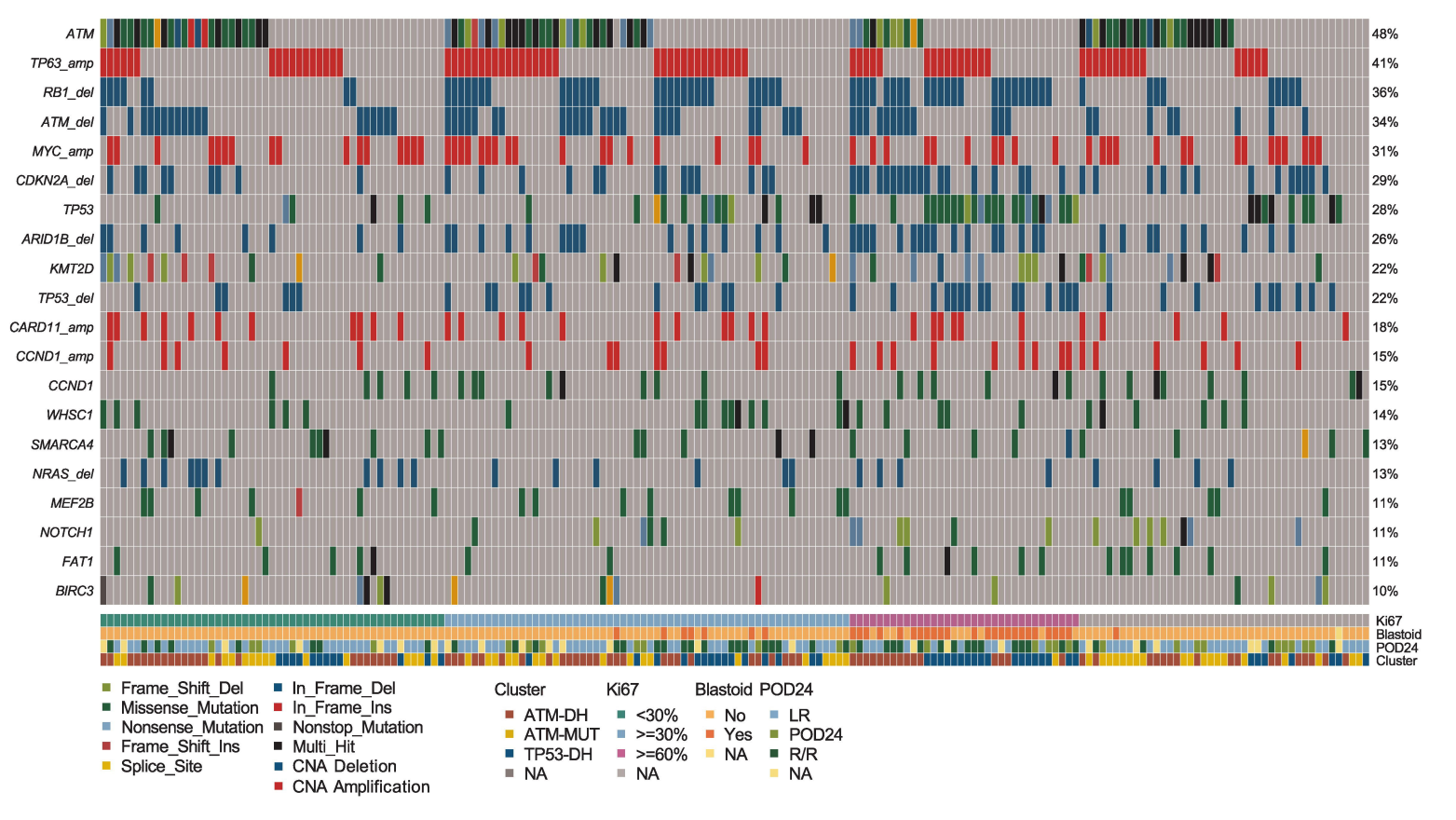
ATM 48%
TP63_amp 41%
RB1_del 36%
ATM_del 34%
MYC_amp 31%
CDKN2A_del 29%
TP53 28%
ARID1B_del 26%
KMT2D 22%
TP53_del 22%
CARD11_amp 18%
CCND1_amp 15%
CCND1 15%
WHSC1 14%
SMARCA4 13%
NRAS_del 13%
MEF2B 11%
NOTCH1 11%
FAT1 11%
BIRC3 10%
Ki67
Blastoid
POD24
Cluster
Frame_Shift_Del
Missense_Mutation
Nonsense_Mutation
Frame_Shift_Ins
Splice_Site
In_Frame_Del
In_Frame_Ins
Nonstop_Mutation
Multi_Hit
CNA Deletion
CNA Amplification
Cluster
ATM-DH
ATM-MUT
TP53-DH
NA
Ki67
<30%
>=30%
>=60%
NA
Blastoid
No
Yes
NA
POD24
LR
POD24
R/R
NA

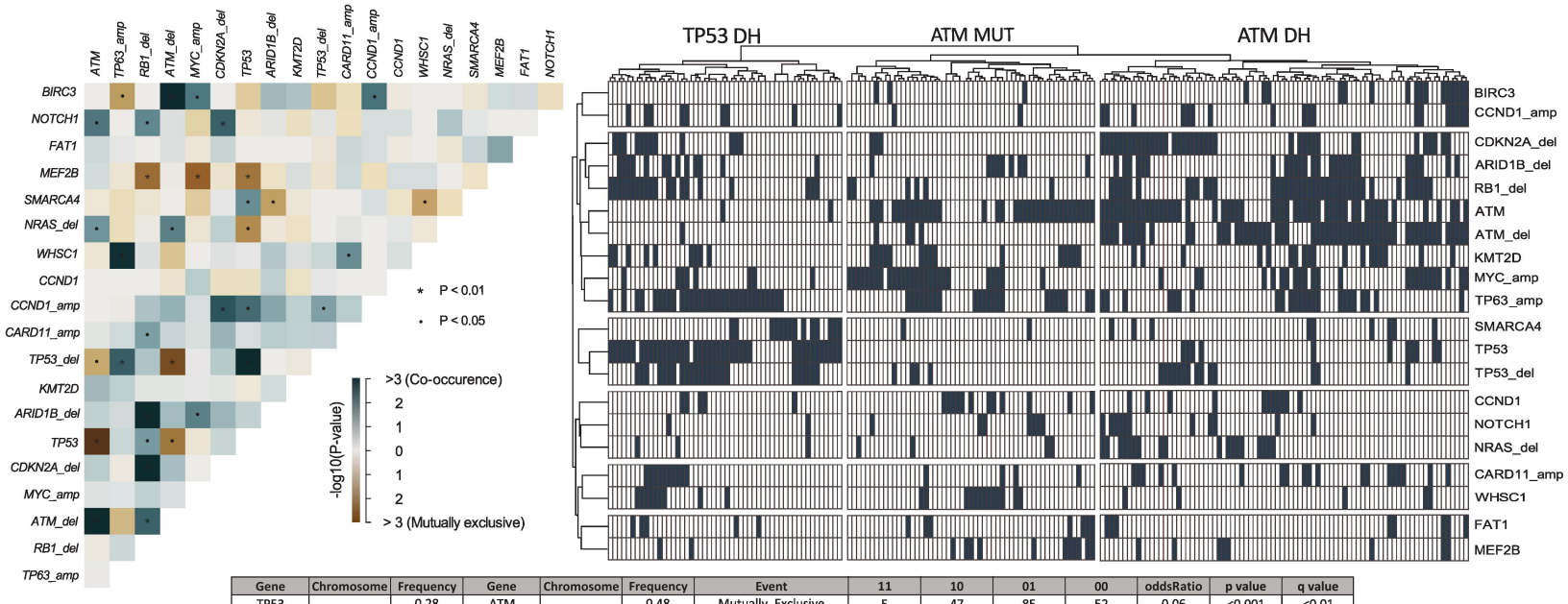

Gene	Chromosome	Frequency	Gene	Chromosome	Frequency	Event	11	10	01	00	oddsRatio	p value	q value
TP53		0.28	ATM		0.48	Mutually_Exclusive	5	47	85	52	0.06	<0.001	<0.01
TP53_del	17p13.1	0.22	TP53		0.28	Co_Occurence	27	15	25	122	8.58	<0.001	<0.01
RB1_del	13q14.2	0.35	ARID1B_del	6q25.3	0.26	Co_Occurence	32	35	17	105	5.53	<0.001	<0.01
ATM_del	11q22.3	0.34	BIRC3		0.10	Co_Occurence	16	47	3	123	13.63	<0.001	<0.01
CDKN2A_del	9p21.3	0.28	RB1_del	13q14.2	0.35	Co_Occurence	33	21	34	101	4.58	<0.001	<0.01
ATM_del	11q22.3	0.34	ATM		0.48	Co_Occurence	42	21	48	78	3.19	<0.001	<0.01
TP63_amp	3q28	0.41	WHSC1		0.14	Co_Occurence	19	59	8	103	4.07	0.001	0.02
ATM_del	11q22.3	0.34	TP53_del	17p13.1	0.22	Mutually_Exclusive	6	57	36	90	0.26	0.003	0.03
MEF2B		0.11	MYC_amp	8q24.21	0.31	Mutually_Exclusive	1	20	58	110	0.09	0.005	0.05
CDKN2A_del	9p21.3	0.28	CCND1_amp	11q13.3	0.15	Co_Occurence	15	39	14	121	3.27	0.006	0.06
MEF2B		0.11	RB1_del	13q14.2	0.35	Mutually_Exclusive	2	19	65	103	0.17	0.007	0.07
TP63_amp	3q28	0.41	TP53_del	17p13.1	0.22	Co_Occurence	25	53	17	94	2.57	0.008	0.07
NOTCH1		0.11	CDKN2A_del	9p21.3	0.28	Co_Occurence	11	9	43	126	3.52	0.009	0.08
ATM_del	11q22.3	0.34	RB1_del	13q14.2	0.35	Co_Occurence	31	32	36	90	2.38	0.009	0.08
MEF2B		0.11	TP53		0.28	Mutually_Exclusive	1	20	51	117	0.11	0.01	0.08

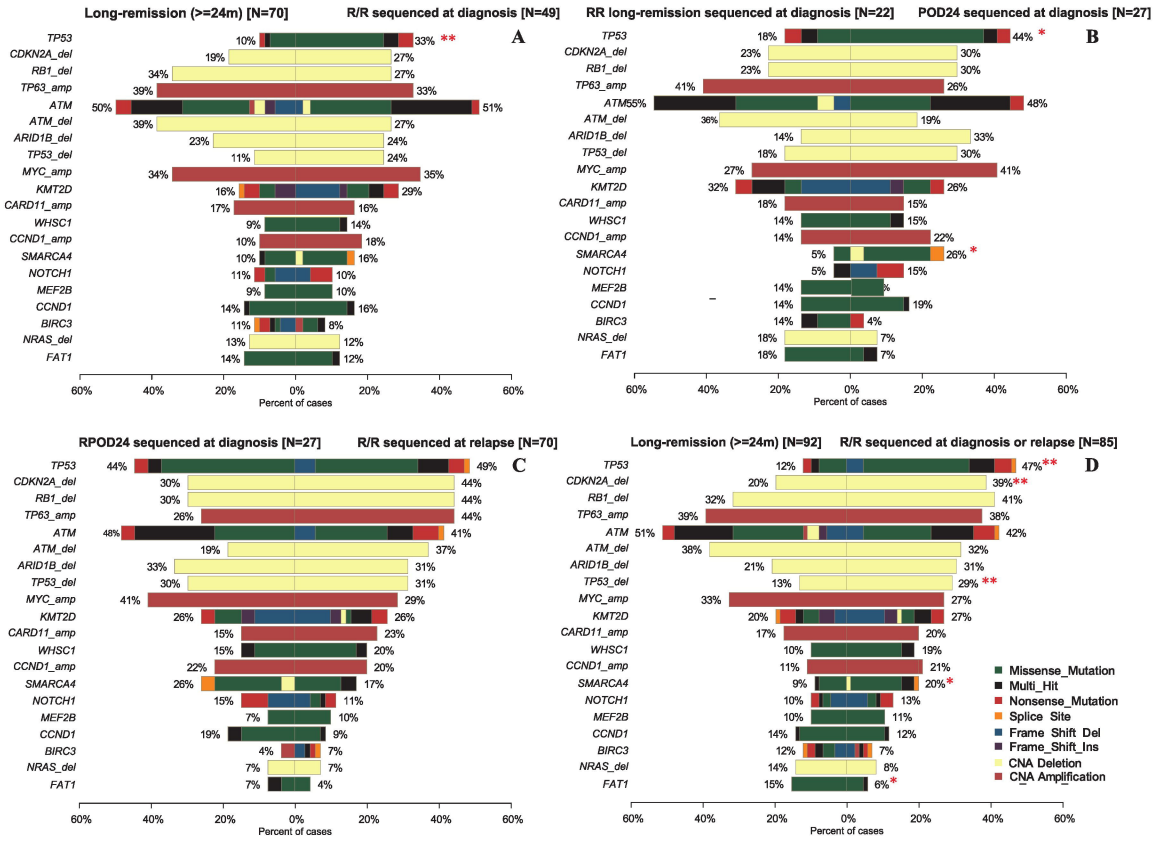
Long-remission (>=24m) [N=70]
R/R sequenced at diagnosis [N=49]
A
TP53 10% 33% **
CDKN2A_del 19% 27%
RB1_del 34% 27%
TP63_amp 39% 33%
ATM 50% 51%
ATM_del 39% 27%
ARID1B_del 23% 24%
TP53_del 11% 24%
MYC_amp 34% 35%
KMT2D 16% 29%
CARD11_amp 17% 16%
WHSC1 9% 14%
CCND1_amp 10% 18%
SMARCA4 10% 16%
NOTCH1 11% 10%
MEF2B 9% 10%
CCND1 14% 16%
BIRC3 11% 8%
NRAS_del 13% 12%
FAT1 14% 12%
60% 40% 20% 0% 20% 40% 60%
Percent of cases
RR long-remission sequenced at diagnosis [N=22]
POD24 sequenced at diagnosis [N=27]
B
TP53 18% 44% *
CDKN2A_del 23% 30%
RB1_del 23% 30%
TP63_amp 41% 26%
ATM 55% 48%
ATM_del 36% 19%
ARID1B_del 14% 33%
TP53_del 18% 30%
MYC_amp 27% 41%
KMT2D 32% 26%
CARD11_amp 18% 15%
WHSC1 14% 15%
CCND1_amp 14% 22%
SMARCA4 5% 26% *
NOTCH1 5% 15%
MEF2B 14% 8%
CCND1 14% 19%
BIRC3 14% 4%
NRAS_del 18% 7%
FAT1 18% 7%
60% 40% 20% 0% 20% 40% 60%
Percent of cases
RPOD24 sequenced at diagnosis [N=27]
R/R sequenced at relapse [N=70]
C
TP53 44% 49%
CDKN2A_del 30% 44%
RB1_del 30% 44%
TP63_amp 26% 44%
ATM 48% 41%
ATM_del 19% 37%
ARID1B_del 33% 31%
TP53_del 30% 31%
MYC_amp 41% 29%
KMT2D 26% 26%
CARD11_amp 15% 23%
WHSC1 15% 20%
CCND1_amp 22% 20%
SMARCA4 26% 17%
NOTCH1 15% 11%
MEF2B 7% 10%
CCND1 19% 9%
BIRC3 4% 7%
NRAS_del 7% 7%
FAT1 7% 4%
60% 40% 20% 0% 20% 40% 60%
Percent of cases
Long-remission (>=24m) [N=92]
R/R sequenced at diagnosis or relapse [N=85]
D
TP53 12% 47% **
CDKN2A_del 20% 39% **
RB1_del 32% 41%
TP63_amp 39% 38%
ATM 51% 42%
ATM_del 38% 32%
ARID1B_del 21% 31%
TP53_del 13% 29% **
MYC_amp 33% 27%
KMT2D 20% 27%
CARD11_amp 17% 20%
WHSC1 10% 19%
CCND1_amp 11% 21%
SMARCA4 9% 20% *
NOTCH1 10% 13%
MEF2B 10% 11%
CCND1 14% 12%
BIRC3 12% 7%
NRAS_del 14% 8%
FAT1 15% 6% *
Missense_Mutation
Multi_Hit
Nonsense_Mutation
Splice_Site
Frame_Shift_Del
Frame_Shift_Ins
CNA Deletion
CNA Amplification
60% 40% 20% 0% 20% 40% 60%
Percent of cases

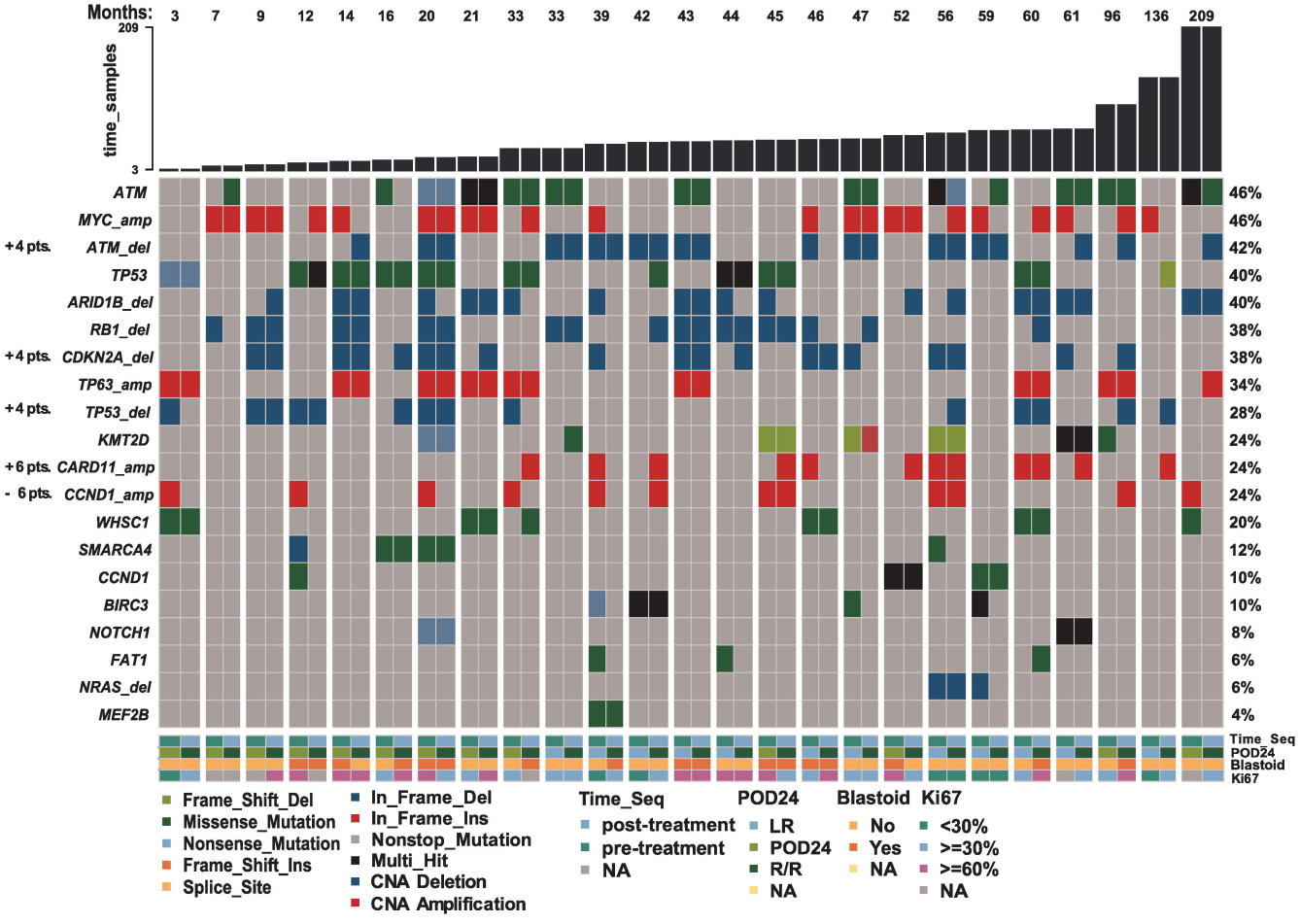
Months: 3 7 9 12 14 16 20 21 33 33 39 42 43 44 45 46 47 52 56 59 60 61 96 136 209
time_samples
209
3
ATM 46%
MYC_amp 46%
+4 pts. ATM_del 42%
TP53 40%
ARID1B_del 40%
RB1_del 38%
+4 pts. CDKN2A_del 38%
TP63_amp 34%
+4 pts. TP53_del 28%
KMT2D 24%
+6 pts. CARD11_amp 24%
- 6 pts. CCND1_amp 24%
WHSC1 20%
SMARCA4 12%
CCND1 10%
BIRC3 10%
NOTCH1 8%
FAT1 6%
NRAS_del 6%
MEF2B 4%
Time_Seq
POD24
Blastoid
Ki67
Frame_Shift_Del
Missense_Mutation
Nonsense_Mutation
Frame_Shift_Ins
Splice_Site
In_Frame_Del
In_Frame_Ins
Nonstop_Mutation
Multi_Hit
CNA Deletion
CNA Amplification
Time_Seq
post-treatment
pre-treatment
NA
POD24
LR
POD24
R/R
NA
Blastoid
No
Yes
NA
Ki67
<30%
>=30%
>=60%
NA

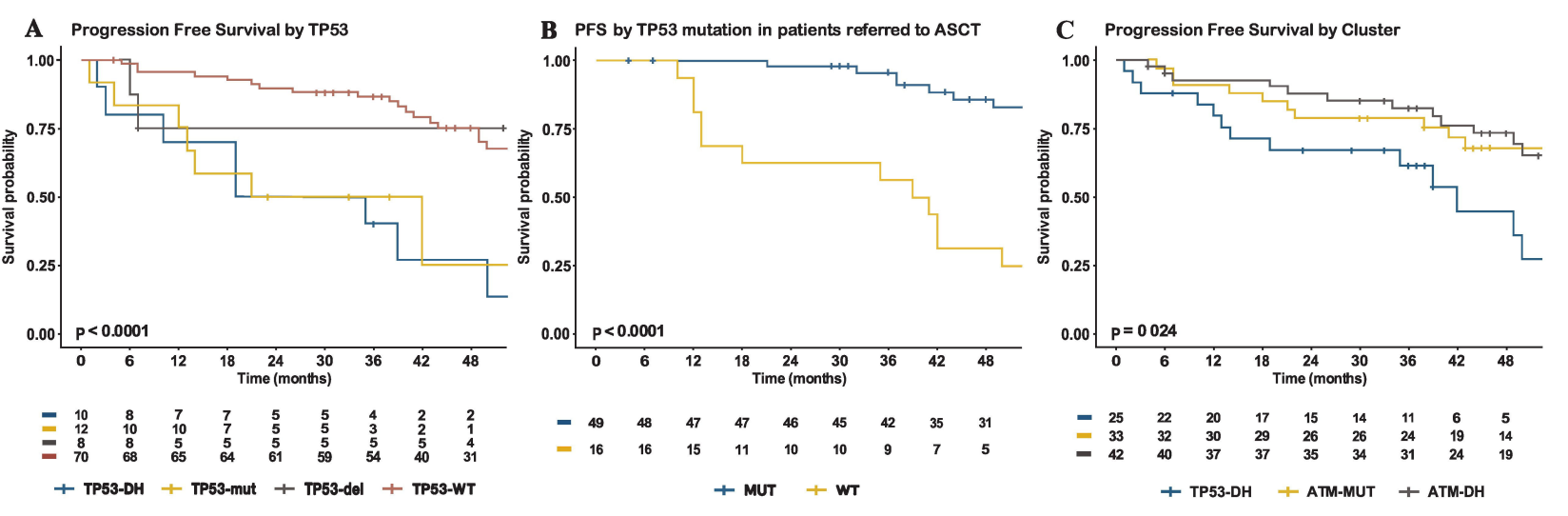
A
Progression Free Survival by TP53
Survival probability
1.00
0.75
0.50
0.25
0.00
p < 0.0001
0 6 12 18 24 30 36 42 48
Time (months)
10 8 7 7 5 5 4 2 2
12 10 10 7 5 5 3 2 1
8 8 5 5 5 5 5 5 4
70 68 65 64 61 59 54 40 31
TP53-DH TP53-mut TP53-del TP53-WT
B
PFS by TP53 mutation in patients referred to ASCT
Survival probability
1.00
0.75
0.50
0.25
0.00
p < 0.0001
0 6 12 18 24 30 36 42 48
Time (months)
49 48 47 47 46 45 42 35 31
16 16 15 11 10 10 9 7 5
MUT WT
C
Progression Free Survival by Cluster
Survival probability
1.00
0.75
0.50
0.25
0.00
p = 0 024
0 6 12 18 24 30 36 42 48
Time (months)
25 22 20 17 15 14 11 6 5
33 32 30 29 26 26 24 19 14
42 40 37 37 35 34 31 24 19
TP53-DH ATM-MUT ATM-DH

SUPPLEMENTARY MATERIALS

Figure S1: Copy Number Alteration (CNA) calling

Figure S2: Example of the effect of heterozygous loci enrichment for CNA calling

Figure S3: Consort Diagram (mutations only)

Figure S4: Genomic landscape of MCL (grouped by Ki67; mutations only)

Figure S5: Genomic landscape at frontline and at later lines of treatment comparing patients with long remission to those with earlier progression of disease

Figure S6: Genomic landscape prior to frontline treatment and at POD (sequential samples; mutations only)

See Supplementary Excel files

Table S1: Gene list - MSK-IMPACT targeted Heme panel

Table S2: CNA SNP validation: Evaluation of CNA calling compared to SNP array (n=18)

Table S3: MUT-CNA Diagnosis vs Relapse - Mutational and CNA landscape pre-treatment and at progression of disease

Table S4: MUT-CNA Ki67 - Mutational and CNA prevalence by Ki67

Table S5: Sequential samples - Copy Number Alteration (CNA) calling

Table S6: MUT-CNA PFS multivariable - Association of mutations and CNA with progression f ree survival - multivariable analysis

Table S7: MUT-CNA OS multivariable - Association of mutations and CNA with overall survival - multivariable analysis

Figure S1: Copy Number Alteration (CNA) calling

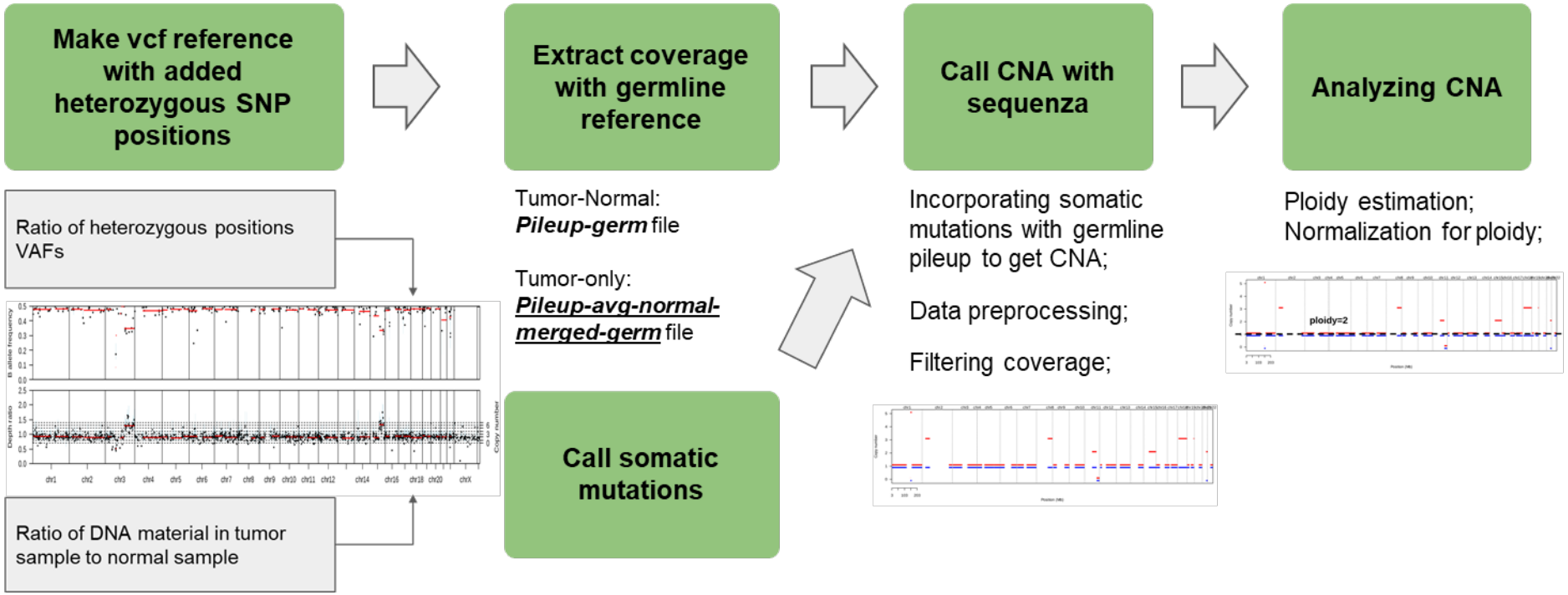

For CNA calling we used a modified algorithm of Sequenza v2.1.2, which was optimized for better filtration (of possible focal false-positive segments in centromere regions), as well as being introduced to the usage of FACETS v0.5.14 SNPs database for better coverage extraction and faster work. However, since all the samples were sequenced on a targeted platform, we faced the problem of lacking heterozygous positions for calling allele-specific CNAs. This issue was solved with the usage of heterozygous germline mutations called by Strelka v2.8.2. Positions of heterozygous mutations were included into individual reference vcf files for each sample, thus enriching the targeted regions and providing us with more statistical information for reliable segmentation and CNA calling.

Figure S2: Example of the effect of heterozygous loci enrichment for CNA calling

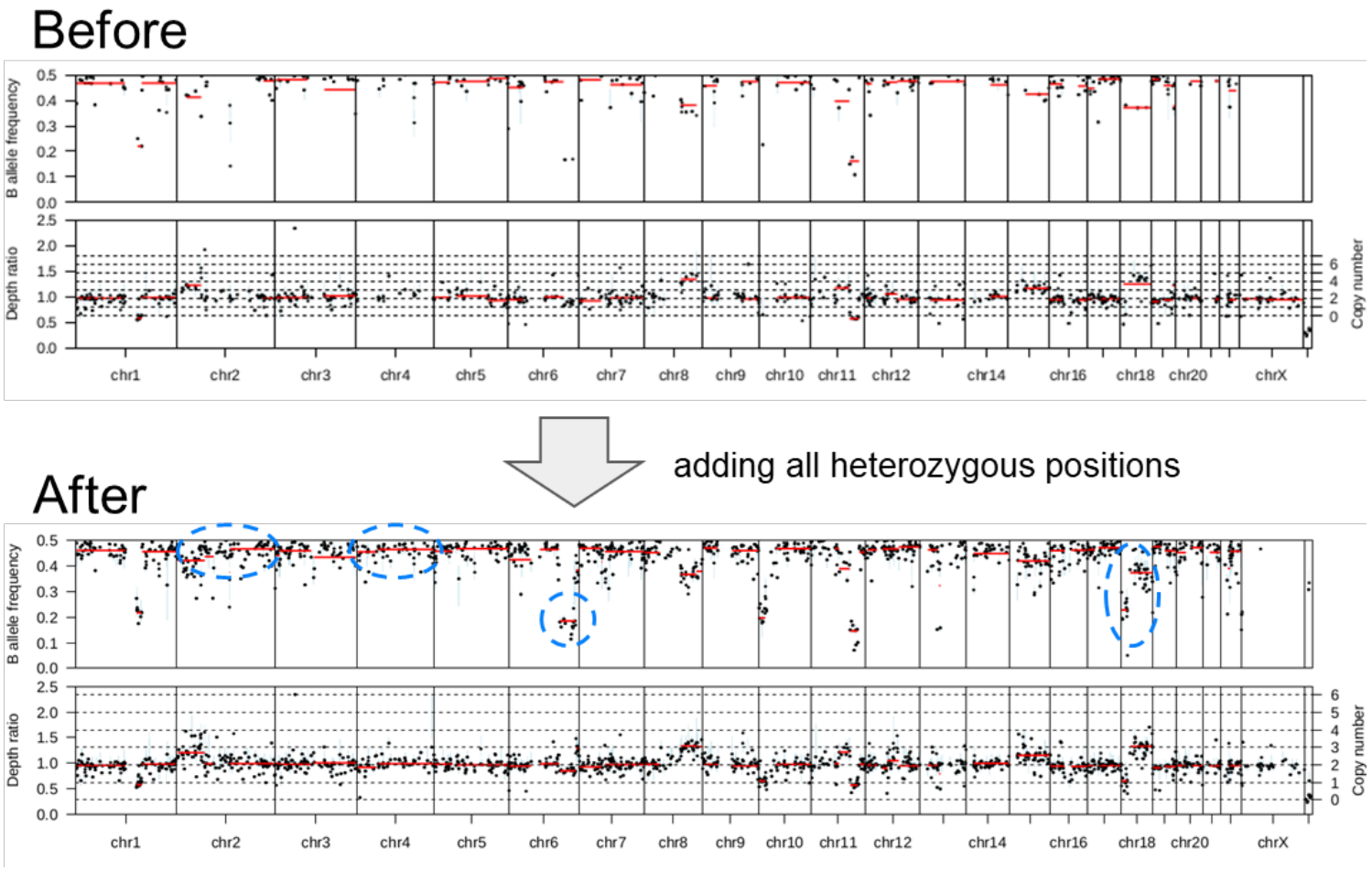

Figure S3: Consort Diagram (mutations only)

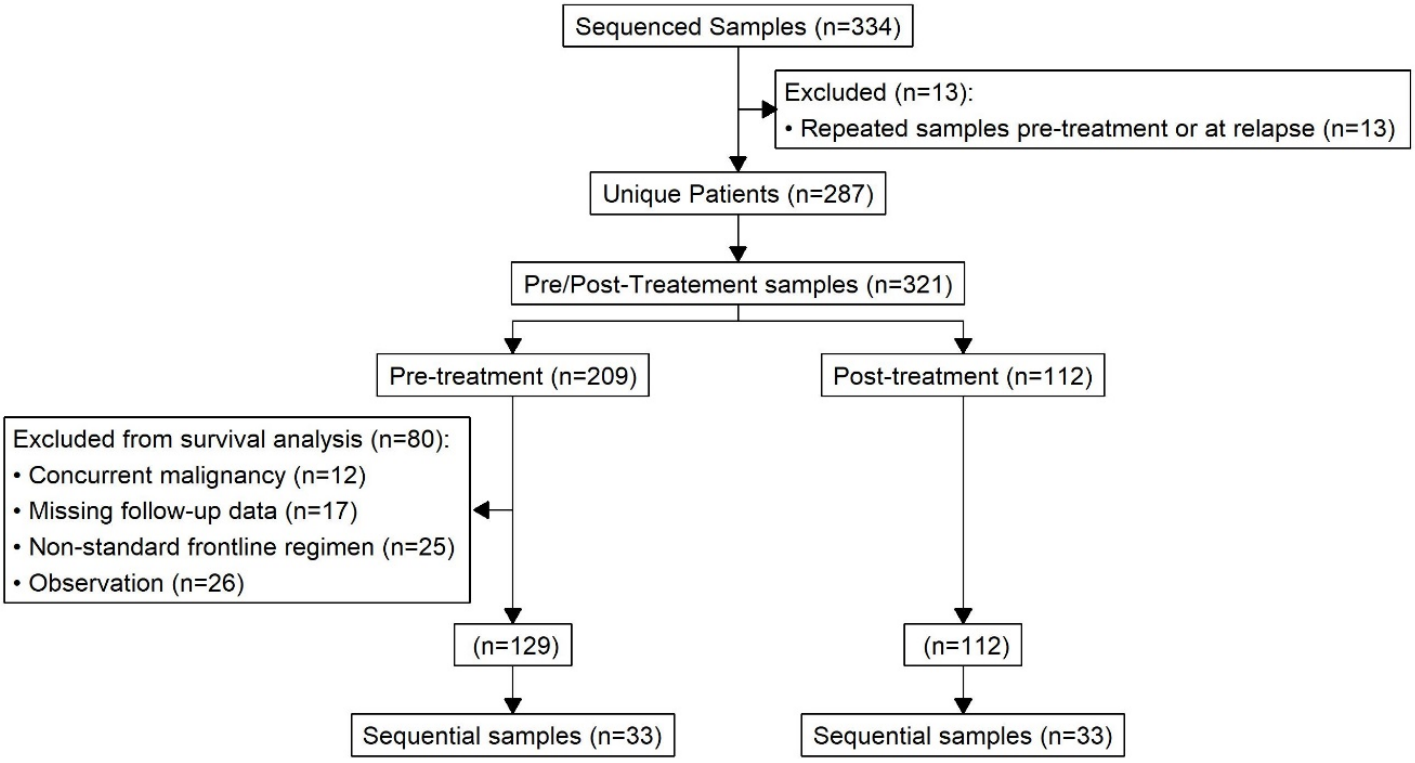

Figure S4: Genomic landscape of MCL (grouped by Ki67; mutations only)

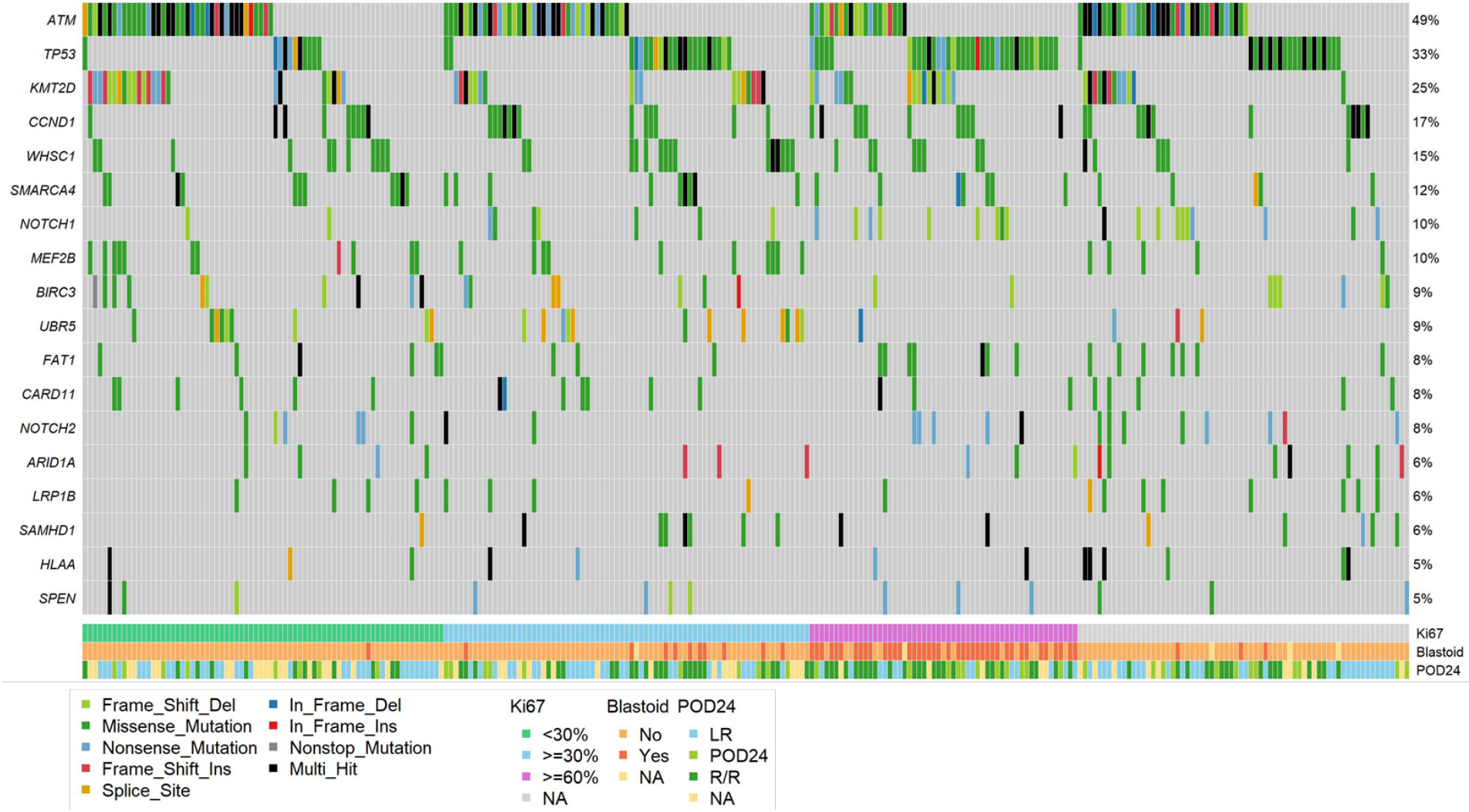

Unique cases only, excluding sequential samples from the same patient.
POD24 – cases sequenced pre-treatment who experienced a POD within ≤24m vs LR patients with a longer remission vs R/R samples sequenced at time of relapse.

Figure S5: Genomic landscape at frontline and at later lines of treatment comparing patients with long remission to those with earlier

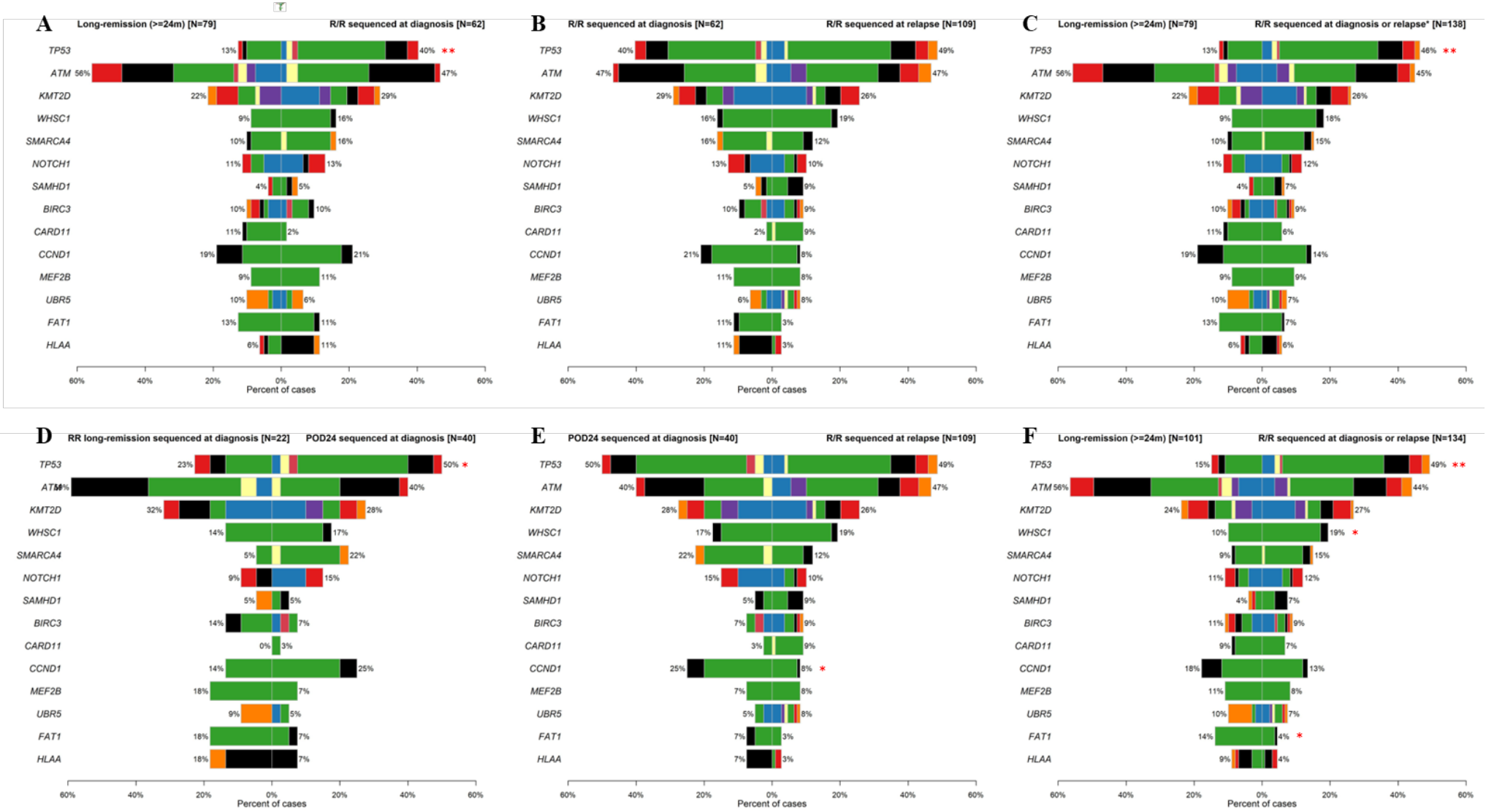

Long Remission – follow-up of at least 24m without POD; Progression – disease relapse at any time (deaths without lymphoma not considered an event); Excluded are 71 samples of patients with insufficient follow-up or not treated with chemoimmunotherapy. (A) Samples prior to frontline therapy comparing patients with a long remission (>24m) to those of patients who experienced a relapse at any time; (B) samples prior to frontline therapy from patients who later experienced a POD compared to samples sequenced at relapse; (C) Samples from patients who experienced a relapse, whether sequenced prior to frontline treatment or at a subsequent line of therapy were enriched for mutations in TP53 (** $p \leq 0.001$). (D) Samples prior to frontline treatment from patients who experienced a POD24 (N=40) had a higher rates of TP53 (* p=0.03; insignificant after correction for FDR) E) samples sequenced at frontline from patients with POD24 were very similar to those sequenced at relapse; (F) Samples from patients sequenced at frontline who later experienced a POD24 and those sequenced at relapse had higher rate of mutations in WHSC1 and lower rate of mutations in FAT1 (* $p \leq 0.05$; insignificant after correction for FDR). Note: plots C&E exclude sequential samples from the same patient.

Figure S6: Genomic landscape prior to frontline treatment and at POD (sequential samples)

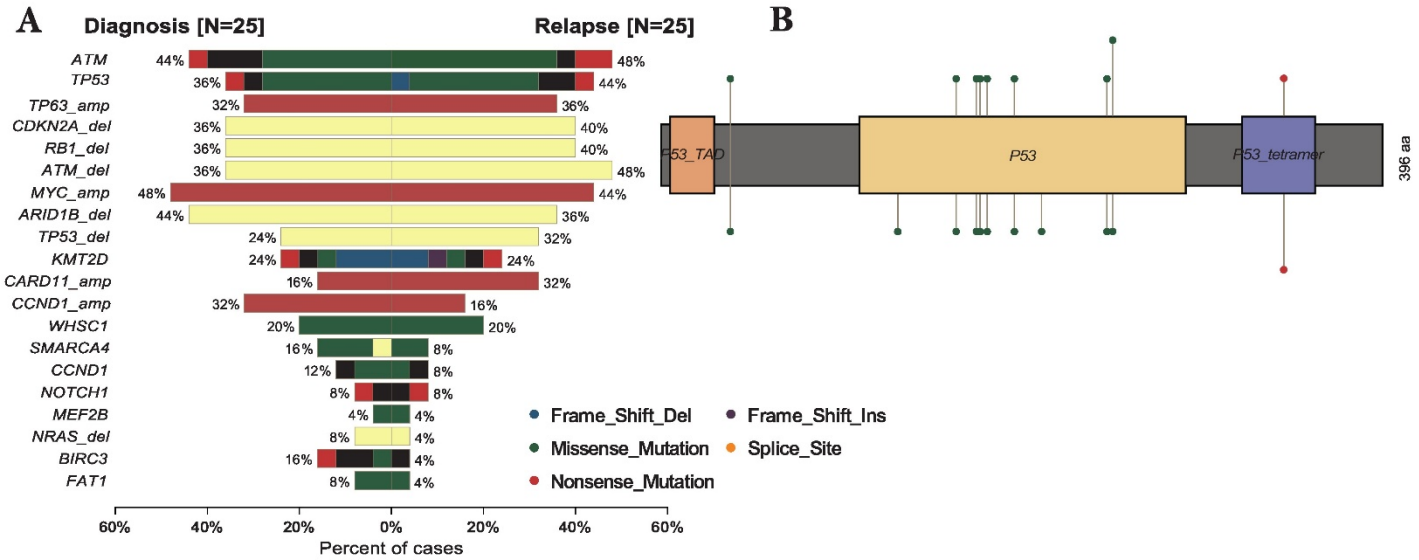

A) Overall rates of genomic alterations comparing paired pre-treatment and at POD samples; C) Lollipop plots of loci of mutations in the TP53 gene in sequential cases sequenced pre-treatment and at POD.

Figure S7: Genomic landscape prior to frontline treatment and at POD (sequential samples; mutations only)

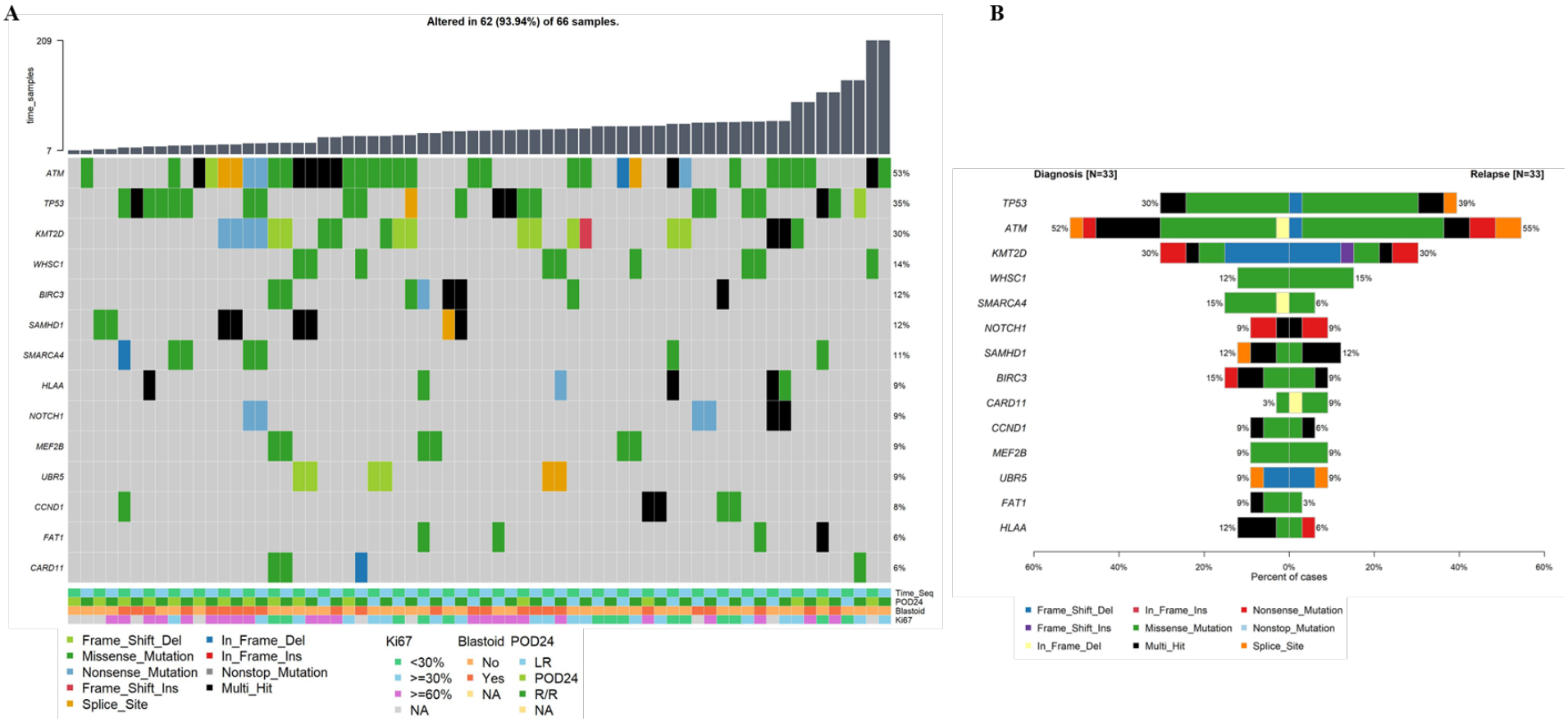

A) Sequential samples where Time_Seq (top_bottom_row) represent the timing of sequencing pre-treament (light-green) or at the time of subsequent treatment; POD24 (second_row) represents whether the first relapse occurred within 24 months (POD24 light-green) or whether the relapse occurred after a longer remission (LR light-blue). Thus, a combination of a light-blue box and a dark-green box on this line indicates a couplet of samples from before frontline treatment and after a considerable remission (the length of time between samples can be inferred from the bars at the top of the plot). Blastoid/Ki67 refers to disease status at the time of sequencing. B) Overall rates of genomic alterations comparing paired pre-treatment and at POD samples.